

Towards a GPU-Parallelization of the neXtSIM-DG Dynamical Core

Robert Jendersie
robert.jendersie@ovgu.de
Institute for Simulation and Graphics
and Institute of Analysis und
Numerics, Otto-von-Guericke
University
Magdeburg, Germany

Christian Lessig
christian.lessig@ecmwf.int
European Centre for Medium-Range
Weather Forecasts
Bonn, Germany

Thomas Richter
thomas.richter@ovgu.de
Institute of Analysis und Numerics,
Otto-von-Guericke University
Magdeburg, Germany

ABSTRACT

The cryosphere plays a significant role in Earth’s climate system. Therefore, an accurate simulation of sea ice is of great importance to improve climate projections. To enable higher resolution simulations, graphics processing units (GPUs) have become increasingly attractive as they offer higher floating point peak performance and better energy efficiency compared to CPUs. However, making use of the theoretical peak performance usually requires more care and effort in the implementation. In recent years, a number of frameworks have become available that promise to simplify general purpose GPU programming. In this work, we compare multiple such frameworks, including CUDA, SYCL, Kokkos and PyTorch, for the parallelization of neXtSIM-DG, a finite-element based dynamical core for sea ice. We evaluate the different approaches according to their usability and performance.

CCS CONCEPTS

- **Computing methodologies** → **Massively parallel algorithms;**
- **Applied computing** → *Earth and atmospheric sciences.*

KEYWORDS

GPU, Heterogeneous computing, Finite elements

ACM Reference Format:

Robert Jendersie, Christian Lessig, and Thomas Richter. 2024. Towards a GPU-Parallelization of the neXtSIM-DG Dynamical Core. In *Proceedings of Platform for Advanced Scientific Computing (PASC)*. ACM, New York, NY, USA, 9 pages. <https://doi.org/10.1145/nnnnnnn.nnnnnnn>

1 INTRODUCTION

Simulations are critical to understand the effects of climate change and to enable stakeholders to mitigate its impact on societies and individuals [14]. An important part of the Earth’s climate system is the cryosphere, which impacts in particular long term processes.

Permission to make digital or hard copies of all or part of this work for personal or classroom use is granted without fee provided that copies are not made or distributed for profit or commercial advantage and that copies bear this notice and the full citation on the first page. Copyrights for components of this work owned by others than ACM must be honored. Abstracting with credit is permitted. To copy otherwise, or republish, to post on servers or to redistribute to lists, requires prior specific permission and/or a fee. Request permissions from permissions@acm.org.

PASC, June 03–05, 2024, Zurich, Switzerland

© 2024 Association for Computing Machinery.

ACM ISBN 978-x-xxxx-xxxx-x/YY/MM. . . \$15.00

<https://doi.org/10.1145/nnnnnnn.nnnnnnn>

The Scale-Aware Sea Ice Project (SASIP)¹ is currently developing the novel sea ice model neXtSIM-DG for climate simulations that aims to both improve the representation of the physical processes and the efficiency and accuracy of the numerical implementation.

An important factor for the fidelity and reliability of climate simulations is the horizontal resolution, with 1 km, convection-resolving simulations being targeted for the next generation of models [4, 26]. The resulting computations necessitate exascale HPC systems with significant GPU-based accelerators [25]. Substantial efforts have hence been devoted to porting components of existing climate models to the GPU [7, 13, 24, 27].

In line with these developments, SASIP aims to substantially increase the resolution of cryosphere simulations in coupled climate models. Its dynamical core builds on a viscous plastic sea ice model with a discretization based on a higher order discontinuous/continuous Galerkin method [23]. Computationally, this leads to a large number of identical per-element operations. This data parallelism make the computations well suited for GPUs, which are built around a data parallel processing model.

In this work, we evaluate different options for the GPU parallelization of the neXtSIM-DG dynamical core. CUDA remains very popular and is the de facto standard for general purpose GPU programming but only works on NVIDIA hardware. Furthermore, it typically implies a dedicated GPU implementation whose development and performance tuning requires substantial effort. For these reasons, different options have emerged that promise greater flexibility and usability. Directive-based GPU programming frameworks such as OpenMP and OpenACC require typically minimal changes to the code but also provide little control and options for performance optimizations. SYCL [30] and Kokkos [32] are frameworks designed for heterogeneous computing that allow to target different compute hardware. A major challenge for these is to attain close-to-optimal performance across different hardware platforms and in particular to efficiently exploit GPU specific features such as shared memory or tensor cores. Another recent alternative are libraries such as jax and PyTorch that were primarily developed for machine learning. Their backends consist of high-performance linear algebra libraries that target different hardwares and that include a compiler to map computations efficiently onto these. Examples for these backends include XLA [1], Triton [31] and TensorRT [21].

Our results show that options such as SYCL and Kokkos still suffer from an unreliable toolchain. Dedicated CUDA code remains a strong baseline with Kokkos providing comparable performance.

¹<https://sasip-climate.github.io>

PyTorch’s new compiler TorchInductor provides a slight performance advantage over hand-written CUDA code. Its usability is currently, however, limited since it is not designed for a stand-alone use in C++, although we show that this is possible.

The remainder of the paper is structured as follows. In Sec. 2 we give a brief overview of the neXtSIM-DG dynamical core. The different GPU implementations of it are detailed in the subsequent Sec. 3. Results are presented in Sec. 4 and directions for future work and a summary is provided in Sec. 5.

2 MODEL DESCRIPTION

The viscous plastic sea ice model by Hibler [12] consists of advection equations for the ice height H and ice concentration A

$$\partial_t H + \text{div}(\mathbf{v}H) = S_H, \quad \partial_t A + \text{div}(\mathbf{v}A) = S_A, \quad (1)$$

and the momentum equation for the two dimensional velocity field

$$\rho_{\text{ice}} H \partial_t \mathbf{v} = \text{div} \boldsymbol{\sigma}(\mathbf{v}, A, H) + F, \quad (2)$$

with the ice density ρ_{ice} and F combining all external forcings. Various material models are discussed in the literature [10] but we focus on the classical viscous-plastic model. Since implicit solvers for this highly non-linear model are costly [18], one often uses an explicit iteration in the sense of a pseudo-time stepping iteration, namely the mEVP solver [6]

$$\boldsymbol{\sigma}^{(p)} = \frac{\alpha}{1+\alpha} \boldsymbol{\sigma}^{(p-1)} + \frac{1}{1+\alpha} \boldsymbol{\sigma}_{vp}(\mathbf{v}^{(p-1)}, A, H), \quad (3)$$

$$\boldsymbol{\sigma}_{vp}(\mathbf{v}, A, H) = \eta(\nabla \mathbf{v} + \nabla \mathbf{v}^T) + \zeta \text{div}(\mathbf{v})I - \frac{P}{2},$$

where the viscosities η, ζ depend on velocity, ice height and ice concentration. The typical solution procedure is thereby as follows: The advection equation (1) is solved with a large time step. The momentum equation (2) and mEVP iteration (3) are then subcycled with a smaller step size. Usually, more than 100 substeps are performed per advection step. The main effort in each case is the evaluation of the non-linear material law, given by $\boldsymbol{\sigma}(\mathbf{v}, A, H)$. Details on the discretization and solution method are given in [23].

2.1 Discretization

The neXtSIM-DG dynamical core [23] discretizes equations (1)-(3) on quadrilateral meshes in spherical coordinates. Discretization of the advection equations is by higher order discontinuous Galerkin methods using a standard upwind scheme. In time, higher order explicit Runge-Kutta methods are used. The velocity is discretized using higher order continuous finite elements and the stress variable is represented in the gradient of the velocity space, which results in a tensor-valued discontinuous Galerkin method.

The mesh is topologically fully structured and the mesh elements are mapped from a reference element onto the computational mesh for better alignment with coastlines and a more equal mesh spacing. This isoparametric element map comes from the same finite element space as the velocity. Details are again given in [23].

3 IMPLEMENTATION

Our work uses the C++ CPU implementation of the NextSim-DG dynamical core [23] as basis for the GPU port and as reference for performance evaluation. The CPU implementation leverages the

	serial [s]	OpenMP [s]	speedup
advection	188.32	34.34	5.48
strain	918.84	185.28	4.96
stress	1741.43	206.36	8.44
divergence	1023.07	170.81	5.99
velocity	728.80	85.73	8.50
total	4653.2	699.75	6.65

Table 1: Runtime of 120 time-steps of the simulation with 2.6×10^5 elements on a 10 core CPU. Except for the advection, all major computations are part of the mEVP iteration which performs 100 sub-steps in each time-step.

linear algebra library Eigen [11], which is highly optimized and, e.g., exploits CPU vector units. Computations consist mostly of a large number of matrix-vector products and component-wise vector operations with small vectors, e.g. of size 8, corresponding to per-element operations in the finite element discretization. Since the vector sizes are known at compile time, the implementation benefits greatly from Eigen’s template-based design. In particular, fixed sized matrices do not require dynamic allocations and operations involving such matrices can be fully unrolled. Furthermore, the use of expression templates in Eigen eliminates unnecessary temporary variables in expressions involving multiple operations.

In Table 1 we show computation times for the different parts of the dynamical core. As can be seen there, the mEVP iteration (middle lines of the table from "strain" to "velocity") takes most of the time, with the stress update in particular being the single most expensive part. Since the stress update also scales well with more cores, it is well suited as computational unit for the evaluation of the different GPU programming frameworks. The computations for the stress update is provided as pseudo code in Listing 1 and the original C++ can be found in Appendix A. While the code is in principle generic in the floating-point type, we use double in all our experiments to ensure correctness.

3.1 OpenACC and OpenMP

A simple approach for moving computations to the GPU is to use a directive based model like OpenACC or OpenMP. Then only small or no changes to the code are required. Targeting C, C++ and Fortran, both OpenACC or OpenMP define directives to annotate loops. These instruct the compiler to offload the computations onto the GPU.

OpenACC or OpenMP differ in how the parallel execution is described. OpenMP is *prescriptive*, meaning that the programmer has to detail how a loop should be parallelized. On the other hand, OpenACC provides a simpler *descriptive* directive that leaves more decisions to the compiler. See [34] for more details on the differences between both approaches. In practice, OpenACC tends to give better performance [33, 34]. However, it has more limited compiler support and except for basic support in GCC, OpenACC can only be used with experimental and commercial compilers that mostly target NVIDIA hardware.

To accelerate our code, we tried three different compilers: GCC-12.2 and NVIDIA HPC-23.5 with support for both OpenMP and OpenACC, and Clang-16.0 which currently only supports OpenMP.

```

1 void StressUpdateHighOrder(Matrix<N,n_S>& S11, Matrix<N,n_S>& S12, Matrix<N,n_S>& S22,
2     const Matrix<N,n_S>& E11, const Matrix<N,n_S>& E12, const Matrix<N,n_S>& E22,
3     const Matrix<N,n_A>& H, const Matrix<N,n_A>& A, double α, double β) {
4     for (i=0; i < N; ++i) { # in parallel
5         Vector<n_G> h = max{0, Hi,*PSI(n_A)}
6         Vector<n_G> a = min{1, max{0, Ai,*PSI(n_A)}}
7         Vector<n_G> e11 = Ei,*11PSI(n_S)
8         Vector<n_G> e12 = Ei,*12PSI(n_S)
9         Vector<n_G> e22 = Ei,*22PSI(n_S)
10
11        Vector<n_G> P = P* · h * exp(-20(1-a))
12        Vector<n_G> D = (Δmin2 + 5/4(Ei,*11 * Ei,*11 + Ei,*22 * Ei,*22) + 3/2 Ei,*11 * Ei,*22 + Ei,*12 * Ei,*12)1/2
13        Vector<n_G> P_D = P/D
14
15        Si,*11 = (1 - α-1)Si,*11 + α-1Mi-1(P_D * (5/8 e11 + 3/8 e22) - 1/2 P)
16        Si,*12 = (1 - α-1)Si,*12 + α-1Mi-1(P_D * 1/4 e12)
17        Si,*22 = (1 - α-1)Si,*22 + α-1Mi-1(P_D * (5/8 e22 + 3/8 e11) - 1/2 P)
18    }
19 }

```

Listing 1: Implementation of the mEVP iteration equation (3). Stress and strain tensor components $S^{11}, S^{12}, S^{22}, E^{11}, E^{12}, E^{22} \in \mathbb{R}^{N \times n_S}$ are stored as matrices where N is the number of elements and n_S the number of local DOF's in the stress space. Ice height and concentration are denoted as $H, A \in \mathbb{R}^{N \times n_A}$, where n_A is the number of local DOFs in the advection space. By $H_{i,*} \in \mathbb{R}^{n_A}$ (and similar for the stress and the strain) we denote the local row vector of the DOFs belonging to element i . The matrices $\text{PSI}(n_A) \in \mathbb{R}^{n_A \times n_G}$ are given at compile time and they evaluate the dG functions in the Gauss points with n_G being the number of Gauss points. The matrices $M_i^{-1} \in \mathbb{R}^{n_S \times n_G}$ are pre-assembled and stored for each element. They represent the local inverse mass matrix scaled with the weights coming from the transformation of the mesh elements. By “*” we denote the element-wise Hadamard product of matrices.

However, we quickly found all three compilers to be ill-suited for our purposes. The NVIDIA compiler refused to compile Eigen code, while GCC and Clang either crashed during compilation or produced a broken program that would crash once executed. A further issue with all but the newest Clang was, that the compilers yielded incorrect memory transfer without a warning or error message. In particular, objects which are not trivially copy-able, such as Eigen matrices with at least one dynamic dimension, are not captured properly. While directives are provided to manually specify the needed buffers, this is cumbersome to do for the complicated template-based Eigen types in use. Furthermore, this voids the main advantage of the directive based approach, namely its simplicity. Use of OpenMP and OpenACC was therefore not pursued further.

3.2 CUDA

The de facto standard for general purpose GPU programming remains CUDA [20], a C++ based language and API developed by NVIDIA. CUDA has a mature ecosystem and gives low level access to the GPU, enabling highly optimized code. However, CUDA is limited to NVIDIA hardware.

Starting with version 3.3, Eigen has limited support for CUDA. In particular, fixed sized matrices can be used in CUDA kernels. This allows us to use the code from Listing 1 largely unchanged. While Eigen's manually vectorized code paths need to be disabled to make it work, we still benefit from Eigen's other features mentioned above such as compile time size-based optimizations and expression

templates. To use Eigen with CUDA, we have to ensure that the required data is available on GPU. For dynamic buffers like S^{11} in the code listing, we simply allocate memory manually and copy it as needed before and after the kernel invocation. Inside the CUDA kernel, an `Eigen::Map` is constructed with

```
auto B = Map<Matrix<N,n>>(buf, N, n);
```

which provides the same interface as the original matrix. For compile time matrices such as `PSI` we use constant memory instead. Advantages of constant memory are that no manual memory management is required, memory access can be faster since it goes through a special cache, and the actual coefficients are available to the compiler, enabling further optimizations. In the original C++ CPU code, the constant matrices are defined as static class members with explicit template specialization to enable selection of the proper matrix for the specified dG-degree at compile time. Since static member variables are not supported in CUDA, we instead declare separate variables and utilize `if constexpr` to achieve the same flexibility for generic code:

```

__constant__ constexpr T PSI_1_1[1] = {1.0};
template<int n, int n_G> __device__ auto PSI() {
    if constexpr (n == 1 && n_G == 1) {
        return Map<const Matrix<T,1,1>>(PSI_1_1);
    }
}

```

optimization	time [s]	speedup
CUDA baseline	0.366	1.0
CUDA shared memory	0.371	0.99
CUDA column-major	0.419	0.87
CUDA on-the-fly map	0.323	1.13
AdaptiveCPP baseline	0.466	1.0
AdaptiveCPP shared memory	0.531	0.88
AdaptiveCPP on-the-fly map	0.375	1.24
Kokkos baseline	0.522	1.0
Kokkos shared memory	0.551	0.95
Kokkos on-the-fly map	0.386	1.35

Table 2: Total time spend on the stress computation for the different implementations on an A100. Each modification is tested independently and speedup is relative to the respective baseline.

Another change to consider when using Eigen on GPU is to set the index type to `int`, since the default 64-bit integers are only emulated on GPUs.

We tried a number of optimizations to speed up the Eigen CUDA code, the results of which are shown in Table 2. Frequently, the bottleneck on the GPU is memory access. One remedy is the manual use of the L1-cache, called *shared memory* in CUDA. Shared between all threads in a thread block, it can significantly speed up reads of data that is needed multiple times and by multiple threads or when scattered memory reads/writes are necessary. In Listing 1, the only data that are used multiple times and by multiple threads are the **PSI** matrices. Only minor changes to the code are needed to load the **PSI** matrices into shared memory before use. However, we see no benefit from this change as shown in Table 2. Access through the constant cache is just as fast for the compile time matrices. Shared memory would therefore only be worth considering in this case if we expect to run out of constant memory in our simulation. While limited to 64 KB, we expect all compile time matrices to fit in constant memory since their size only depends on the local degrees of freedom of the discretization.

Another potential avenue to accelerate memory accesses is to carefully prepare the layout of data. For the C++ CPU code, variables such as S^{11} are stored in row-major order, meaning that coefficients belonging to the same cell are continuous in memory. This locality is beneficial both for effective cache usage and for vectorized memory accesses. On the GPU the most efficient way to access global memory is through *coalesced* reads whereby neighboring threads access neighboring addresses. Since each thread processes one cell, this can be achieved by storing variables in column-major order. Nonetheless, as we can see in Table 2, the switch to column-major storage order for all fields causes a measurable slowdown. An investigation with a profiler revealed that the change does improve the memory access patterns as intended. The number of excessive sectors loaded from global memory decrease from 59% for the row-major version to just 2%. However, this potential advantage is negated by the cache, which is used to greater extent by the row-major version and the latter code is faster overall.

A third option to reduce global memory accesses is to trade off reads with more computations. This is beneficial when the code is

memory-bound, as is often the case on the GPU, especially with classical linear algebra [9]. In our code, the I/O can be reduced by re-computing the inverse parametric map M^{-1} , which depends only on the geometry of the mesh and compile time constants. In particular, each matrix has a size of $n_S \times n_G$ while each mesh cell is fully described by 4 vertices with 2 values each. So, disregarding constants, even for a small dG-degree such as $n_G = 3$, fewer reads are required if we compute the matrices on-the-fly. Upon closer inspection, we also find that when stored in column-major order, vertex reads are coalesced while reads to M^{-1} are not, due to the fact that M^{-1} is implemented as an array of matrices. Since the Eigen matrix type only deals with two dimensions, adjusting the storage order of M^{-1} to allow for coalesced accesses would be difficult. Testing on an A100 GPU, we find that the on-the-fly map computation indeed delivers a speedup of 13%.

3.3 SYCL

SYCL is an open standard for heterogeneous computing developed by the Khronos group. With its most recent release SYCL 2020, the standard proposes a high-level API extending C++17 that allows the same code to run on various devices such as CPUs, GPUs and FPGAs. There are currently two major implementations of the standard, both of which are open source and based on LLVM. Development of AdaptiveCPP [2], previously known as hipSYCL and OpenSYCL, is lead by Heidelberg University. While various backends are available, the focus is on NVIDIA and AMD GPUs. The other major implementation is Data Parallel C++ (DPC++), developed by Intel. DPC++ primarily targets Intel CPUs, GPUs and FPGAs.

SYCL builds on top of standard C++ to minimize the effort of adapting existing code. However, the SYCL standard forbids recursion and function pointers in kernel code [29], both of which are used in Eigen’s expression templates. Albeit these function calls should be entirely inlined in the compiled code, DPC++ does not allow one to compile the neXtSIM-DG code because of these issues. AdaptiveCPP requires more effort for setup but the tool chain compiles Eigen. We therefore limit our investigations to AdaptiveCPP in the following.

SYCL automates device memory management and movement between host and device but it needs to be declared which memory will be used in a kernel. In particular, a *buffer* needs to be defined, pointing to already allocated memory on the host. Then, a *command group* is created which collects all information needed to run a task in parallel. Inside the command group, *accessors* allow us to explicitly describe which buffers need to be accessed and how, i.e. read or write. Once put in a *queue*, the SYCL runtime uses these memory requirements as well as optional dependencies on other command groups to select the best suited memory region to perform needed memory transfers and to schedule the execution. Inside the command group, we can declare a parallel for-loop and construct Eigen maps analogous to CUDA with pointers provided by the accessors.

In principal, we can attempt the same optimizations as with the CUDA code. While shared memory did not help in the case of CUDA, it is still of interest to see how its introduction affects the SYCL implementation, since memory management works differently. To

access *local memory* in SYCL, which is the name used for CUDA’s shared memory, we have to declare a *local_accessor* in the command buffer. In addition, local memory only makes sense in the context of thread blocks, so we need to use a more complicated for-loop which makes thread blocks explicit. Unfortunately, such a construct is known to perform far worse on CPU than a simple loop and work on reducing this gap is an active area of research [19]. Therefore, if the code is to be run both on CPU and GPU, local memory should be introduced only in code paths specialized for the GPU. For the code snippet under study, this additional effort was not considered worthwhile. Returning to Table 2 we see using shared memory makes the kernel moderately slower. On the other hand, computing M^{-1} on-the-fly leads to a more substantial speedup than in CUDA.

3.4 Kokkos

Kokkos is another programming model to enable heterogeneous computing in modern C++, currently with support for CPU as well as NVIDIA and AMD GPUs. Kokkos is developed as part of the Exascale Computing Project by the US Department of Energy. The main difference to SYCL is that Kokkos is a library while SYCL needs to be integrated into the compiler. The library-based approach greatly simplifies deployment of projects using Kokkos but potentially limits optimizations and some features.

Kokkos consists of macros and wrappers that provide a unified API for the different backends with the final code being processed by the chosen compiler. Therefore, we can once again use the same code, knowing already that it works in CUDA, and we can expect few differences to the pure CUDA implementation. The primary mechanism to manage memory in Kokkos are *Views*, which are basically a shared pointer to a multi-dimensional array. Commonly, both a device view and a mirrored host view are created to facilitate data transfers. For our use case, it is possible to create a view on already allocated memory with the *Unmanaged* trait. However, because this trait is part of the type, its introduction may lead to unnecessary copies during an execution on CPU. Since in general the device view cannot be unmanaged as it needs its own buffer, copies between the mirrored views will be performed regardless of whether they already reside in the same memory space. This aside, once copied, data is accessible in the kernel through the device view and we can use the underlying pointer to create an Eigen map in the same manner as in CUDA.

Possible code optimizations in Kokkos are similar to those available in SYCL. The L1-cache, called *scratch memory* in Kokkos, can be accessed by specifying a *TeamPolicy* with a thread block size instead of using a simple parallel for-loop. Here a nuisance of the library becomes apparent as the total scratch memory needed for a particular kernel has to be set manually. Furthermore, parallelism described with explicit thread blocks has the same downside as in SYCL, namely that it leads to strongly degraded CPU performance. In our tests, recorded in Table 2, we find that usage of scratch memory introduces a small overhead in Kokkos. On the fly map-computation is, once more, beneficial and it results in a large speedup of 35%.

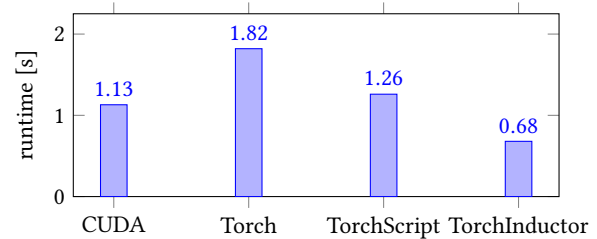


Figure 1: Total time spend on the stress computation for the different PyTorch variants and the optimized CUDA implementation on a NVIDIA RTX 3090.

3.5 PyTorch

PyTorch [22] is one of the most popular libraries for machine learning [3]. It consists of a simple-to-use Python frontend library and a high-performance C++ backend that has a dedicated compiler to optimize code execution and maps execution for different hardware such as CPUs, GPUs, and TPUs.

To make effective use of PyTorch and the optimizations it implements, we have to reformulate our computations in terms of large tensors. For this, we remove the main loop in Line 4 and treat the element dimension N as the batch dimension of variable size. The matrix-vector products become matrix-matrix products and element-wise operations remain unchanged. Some care is necessary to perform the products with the per-element inverse maps, e.g. Line 16. Since we have a third dimension in M^{-1} , this is not a standard matrix-matrix product. However, we can map this operation to a batched matrix-matrix multiplication by adding a dimension of size 1 to the second argument and removing it again afterwards (squeezing in PyTorch terminology).

To integrate the PyTorch code into our C++ simulation we have multiple options. With minor syntactic changes compared to the Python version, we can implement the computations directly with PyTorch’s C++ API. However, this is sub-optimal since each operation is executed as a separate kernel with no kernel-fusion taking place resulting in many reads and writes of the same data. A second option is to define the computation as a PyTorch model in Python. This model can be exported as *TorchScript* and loaded in C++. Part of the C++ runtime is a just-in-time compiler which attempts to optimize the model execution on repeated use. However, more recent efforts to accelerate models have been focused on *TorchDynamo*, a compiler first released with PyTorch 2.0 in March 2023. While the front-end of TorchDynamo is written in Python, various backends are available, some of which can be used without the Python runtime. Most promising among those we tested is the builtin *TorchInductor* which leverages the compiler Triton [31] to produce highly optimized fused-matrix multiplications [28]. In particular, PyTorch 2.2 allows TorchInductor to generate a C++ wrapper function for the entire model which can then be integrated into C++ code with a few modifications. References to the Python runtime need to be removed and the arguments given to the model have to be reorganized.

We compare the three proposed variants to integrate the PyTorch model into C++ in Fig. 1. Albeit they use the same tensor primitives,

the native C++ interface is considerably slower than TorchScript. The new compiler, TorchInductor, with its Triton optimized kernels, is significantly faster than the alternatives. In fact, at least on the RTX 3090, TorchInductor even outperforms the native CUDA code by a significant margin.

4 NUMERICAL EXPERIMENTS

To analyze the performance of our implementations, we use the established VP benchmark of a moving cyclone over a sea ice region [17]. The original C++ CPU version of the code has already been validated on this benchmark, see [23]. We can therefore ensure the correctness of our implementations by comparing to the CPU version. For time measurements, we simulate a duration of 1 h, which requires 30 advection steps and 3,000 stress updates.

In the current GPU implementations, significant time is required to transfer memory between host and device. Nonetheless, we focus on the kernel execution times in the following since the final objective of our work is a full GPU implementation of the dynamical core. While transfers are still necessary for coupling with other models, the major effort of simulating the sea-ice dynamics is in the mEVP iteration. To ensure accurate timings, synchronization barriers are inserted as needed before and after the kernel invocation. In SYCL memory transfers are implicit, so we rely on the builtin profiling instead. Experiments are conducted in the following environment:

- 2× AMD EPYC Rome 7402 CPU, 2 × 24 cores @ 2.8 GHz
- NVIDIA A100 GPU, 40 GB HBM2e
- GCC-12.3
- CUDA 12.2
- Kokkos 4.1.0
- AdaptiveCPP 23.10.0 based on Clang-17.04
- PyTorch 2.2 Nightly (24-November-2023)

Of particular importance for coupled climate simulations is the performance scaling as a function of grid resolution and hence problem size. With a fixed domain size of 512 km, we reduce the resolution from 4 km to 0.25 km, which corresponds to an increase in the number of elements from 1.6×10^4 to 1.7×10^7 (i.e. one has a quadratic scaling in the resolution). In Fig. 2 we compare the best implementation for each approach as a function of elements. For CUDA, Kokkos and AdaptiveCPP, we compute the inverse maps on-the-fly. In case of Kokkos and AdaptiveCPP, the simple for-loop is used to run the update in parallel, which also makes the switch to CPU viable. For PyTorch, we take the implementation generated by TorchInductor.

Our CUDA implementation delivers a significant speedup over the OpenMP CPU reference implementation. For the smallest problem with 1.6×10^4 elements, CUDA is 3 times faster, scaling up to 6.4 for 1.7×10^7 elements. Kokkos asymptotically performs the same as CUDA on GPU and as OpenMP on CPU. This is to be expected since the very same compilers (NVCC and GCC) are used by Kokkos and only memory buffers and kernel dispatch are abstracted. On small problems, Kokkos overhead makes it 50% slower than CUDA but, surprisingly, the CPU version is slightly faster than raw OpenMP for the same number of elements. AdaptiveCPP scales worse than the other GPU accelerated codes, being 70% slower for the largest problem tested. However, it still provides a significant improvement over the CPU OpenMP version. The good performance for small

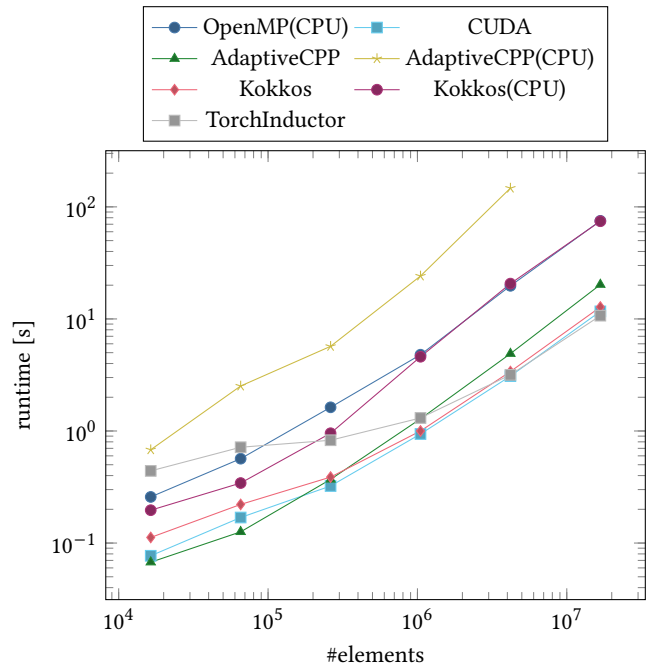


Figure 2: Timings of the stress update using the best performing version for each framework. The size of the mesh cells size is scaled from 4 km to 0.25 km while keeping the domain size constant to increase the number of elements.

numbers is likely just an artifact from the differing time measuring method. On the CPU side, we could not get AdaptiveCPP to run properly. Best performance was achieved with a restriction to just 24 threads, indicating that the available CPUs are not utilized properly. While the documentation mentions possible user errors when running the CPU backend, we were unable to obtain stable results on three different systems, illustrating a greater difficulty in using the framework. Finally, the PyTorch implementation shows the greatest variance as a function of resolution. Slower even than OpenMP on small problems, it scales very well, outperforming native CUDA code beyond 5×10^5 elements. On the largest problem size we measure a speedup of 9% over CUDA. The poor performance on smaller problems and the discrepancy to the results from Fig. 1, obtained on a RTX 3090, warrant further investigation. One important aspect is likely the very large difference in double-precision performance between the RTX 3090. In particular, with a difference in peak double-precision performance by a factor of 17 (A100 without Tensor Cores 9.7 TFLOPS; RTX 3090 0.56 TFLOPS), the RTX 3090 is compute-bound in our workload while the A100 is memory-bound.

5 CONCLUSION

We implemented and analyzed different options for the GPU parallelization of the neXtSIM-DG dynamical core. Our results show that CUDA remains the most reliable option both in term of performance and the toolchain. With the CUDA support of Eigen, we were also able to use the CPU C++ code essentially without modifications in

CUDA, Kokkos and SYCL offer a more advanced programming models but this comes overall with reduced performance. Furthermore, using dedicated GPU features such as shared memory leads to code that is very inefficient on the CPU, breaking the promise of the heterogeneous computing paradigm. SYCL also suffers from immature implementations. Interestingly, PyTorch provides the fastest code for a fine mesh resolution. It outperforms even native CUDA, likely through features such as tensor fusion that are difficult to realize in handwritten code. An improved workflow is, however, required to make it usable in applications.

In future work, we want to investigate more diverse compute hardware, e.g. AMD GPUs and ARM processors and also the use of multiple GPUs. We also want to further study the PyTorch version, for example the performance of the CPU backend and single or mixed precisions which is intrinsically supported by it. Another advantage of the PyTorch backend is that automatic differentiation is immediately available. This is of great relevance for hybrid methods that combine a conventional discretization with a machine learning component, e.g. [5, 8, 15, 16].

6 CODE AVAILABILITY

The project neXtSIM-DG is under active development and hosted on GitHub (<https://github.com/nextsimhub/nextsimdg>). The self contained repository with the GPU implementations and experiments described in this paper is available at https://kosinus.math.uni-magdeburg.de/Thandurriel/dynamical_core.

7 ACKNOWLEDGMENTS

This project is supported by Schmidt Futures – a philanthropic initiative that seeks to improve societal outcomes through the development of emerging science and technologies.

REFERENCES

- [1] 2023. XLA: an open-source machine learning compiler. <https://github.com/openxla/xla> [accessed 28-November-2023].
- [2] Aksel Alpay and Vincent Heuveline. 2023. One Pass to Bind Them: The First Single-Pass SYCL Compiler with Unified Code Representation Across Backends. In *International Workshop on OpenCL*. ACM. <https://doi.org/10.1145/3585341.3585351>
- [3] Mohamed Raed El aoun, Lionel Nganyewou Tidjon, Ben Rombaut, Foutse Khomh, and Ahmed E. Hassan. 2022. An Empirical Study of Library Usage and Dependency in Deep Learning Frameworks. <https://doi.org/10.48550/ARXIV.2211.15733>
- [4] Peter Bauer, Bjorn Stevens, and Wilco Hazeleger. 2021. A digital twin of Earth for the green transition. *Nature Climate Change* 11, 2 (2021), 80–83. <https://doi.org/10.1038/s41558-021-00986-y>
- [5] Mario Christopher Bedrunka, Dominik Wilde, Martin Kliemank, Dirk Reith, Holger Foysi, and Andreas Krämer. 2021. *Lettuce: PyTorch-Based Lattice Boltzmann Framework*. Springer International Publishing, 40–55. https://doi.org/10.1007/978-3-030-90539-2_3
- [6] Sylvain Bouillon, Thierry Fichet, Vincent Legat, and Gurvan Madec. 2013. The elastic–viscous–plastic method revisited. *Ocean Modelling* 71 (nov 2013), 2–12. <https://doi.org/10.1016/j.ocemod.2013.05.013>
- [7] Kai Cao, Qizhong Wu, Lingling Wang, Nan Wang, Huaqiong Cheng, Xiao Tang, Dongqing Li, and Lanning Wang. 2023. GPU-HADVPPM V1.0: a high-efficiency parallel GPU design of the piecewise parabolic method (PPM) for horizontal advection in an air quality model (CAMx V6.10). *Geoscientific Model Development* 16, 15 (aug 2023), 4367–4383. <https://doi.org/10.5194/gmd-16-4367-2023>
- [8] Nestor Demeure, Theodore Kisner, Reijo Keskitalo, Rollin Thomas, Julian Borrill, and Wahid Bhimji. 2023. High-level GPU code: a case study examining JAX and OpenMP. In *Proceedings of the SC '23 Workshops of The International Conference on High Performance Computing, Network, Storage, and Analysis (SC-W 2023)*. ACM. <https://doi.org/10.1145/3624062.3624186>
- [9] Saumay Dubish, Vijay Nagarajan, and Nigel Topham. 2017. Evaluating and mitigating bandwidth bottlenecks across the memory hierarchy in GPUs. In *2017 IEEE International Symposium on Performance Analysis of Systems and Software (ISPASS)*. IEEE. <https://doi.org/10.1109/ispass.2017.7975295>
- [10] D.L. Feltham. 2008. Sea Ice Rheology. *Annual Review of Fluid Mechanics* 40 (2008), 91–112. <https://doi.org/10.1146/annurev.fluid.40.111406.102151>
- [11] Gaël Guennebaud, Benoît Jacob, et al. 2010. Eigen v3. <http://eigen.tuxfamily.org>.
- [12] W. D. Hibler. 1979. A Dynamic Thermodynamic Sea Ice Model. *Journal of Physical Oceanography* 9, 4 (jul 1979), 815–846. [https://doi.org/10.1175/1520-0485\(1979\)009<0815:adtsim>2.0.co;2](https://doi.org/10.1175/1520-0485(1979)009<0815:adtsim>2.0.co;2)
- [13] Olawale James Ikuyajolu, Luke Van Roekel, Steven R. Brus, Erin E. Thomas, Yi Deng, and Sarat Sreepathi. 2023. Porting the WAVEWATCH III (v6.07) wave action source terms to GPU. *Geoscientific Model Development* 16, 4 (mar 2023), 1445–1458. <https://doi.org/10.5194/gmd-16-1445-2023>
- [14] Christian Jakob, Andrew Gettelman, and Andrew Pitman. 2023. The need to operationalize climate modelling. *Nature Climate Change* 13, 11 (2023), 1158–1160. <https://doi.org/10.1038/s41558-023-01849-4>
- [15] Dmitrii Kochkov, Jamie A. Smith, Ayya Alieva, Qing Wang, Michael P. Brenner, and Stephan Hoyer. 2021. Machine learning–accelerated computational fluid dynamics. *Proceedings of the National Academy of Sciences* 118, 21 (May 2021). <https://doi.org/10.1073/pnas.2101784118>
- [16] Dmitrii Kochkov, Janni Yuval, Ian Langmore, Peter Norgaard, Jamie Smith, Griffin Mooers, James Lottes, Stephan Rasp, Peter Düben, Milan Klöwer, Sam Hatfield, Peter Battaglia, Alvaro Sanchez-Gonzalez, Matthew Willson, Michael P. Brenner, and Stephan Hoyer. 2023. Neural General Circulation Models. arXiv:2311.07222 [physics.ao-ph]
- [17] C. Mehlmann, S. Danilov, M. Losch, J. F. Lemieux, N. Hutter, T. Richter, P. Blain, E. C. Hunke, and P. Korn. 2021. Simulating Linear Kinematic Features in Viscous-Plastic Sea Ice Models on Quadrilateral and Triangular Grids With Different Variable Staggering. *Journal of Advances in Modeling Earth Systems* 13, 11 (Oct. 2021). <https://doi.org/10.1029/2021ms002523>
- [18] C. Mehlmann and T. Richter. 2017. A modified global Newton solver for viscous-plastic sea ice models. *Ocean Modelling* 116 (2017), 96–107. <https://doi.org/10.1016/j.ocemod.2017.06.001>
- [19] Joachim Meyer, Aksel Alpay, Sebastian Hack, Holger Fröning, and Vincent Heuveline. 2023. Implementation Techniques for SPMD Kernels on CPUs. In *International Workshop on OpenCL (IWOCCL '23)*. ACM. <https://doi.org/10.1145/3585341.3585342>
- [20] NVIDIA. 2023. CUDA C++ Programming Guide. <https://docs.nvidia.com/cuda/cuda-c-programming-guide/index.html> [accessed 28-November-2023].
- [21] NVIDIA. 2023. TensorRT: an SDK for high-performance deep learning inference. <https://developer.nvidia.com/tensorrt> [accessed 28-November-2023].
- [22] Adam Paszke, Sam Gross, Francisco Massa, Adam Lerer, James Bradbury, Gregory Chanan, Trevor Killeen, Zeming Lin, Natalia Gimelshein, Luca Antiga, Alban Desmaison, Andreas Kopf, Edward Yang, Zachary DeVito, Martin Raison, Alykhan Tejani, Sasank Chilamkurthy, Benoît Steiner, Lu Fang, Junjie Bai, and Soumith Chintala. 2019. PyTorch: An Imperative Style, High-Performance Deep Learning Library. In *Advances in Neural Information Processing Systems 32*, H. Wallach, H. Larochelle, A. Beygelzimer, F. d’Alché Buc, E. Fox, and R. Garnett (Eds.). Curran Associates, Inc., 8024–8035. <http://papers.nips.cc/paper/9015-pytorch-an-imperative-style-high-performance-deep-learning-library.pdf>
- [23] Thomas Richter, Véronique Dansereau, Christian Lessig, and Piotr Minakowski. 2023. A dynamical core based on a discontinuous Galerkin method for higher-order finite-element sea ice modeling. *Geoscientific Model Development* 16, 13 (jul 2023), 3907–3926. <https://doi.org/10.5194/gmd-16-3907-2023>
- [24] Jeremy A. Sauer and Domingo Muñoz-Esparza. 2020. The FastEddy® Resident-GPU Accelerated Large-Eddy Simulation Framework: Model Formulation, Dynamical-Core Validation and Performance Benchmarks. *Journal of Advances in Modeling Earth Systems* 12, 11 (nov 2020). <https://doi.org/10.1029/2020ms002100>
- [25] Christoph Schär, Oliver Fuhrer, Andrea Arteaga, Nikolina Ban, Christophe Charpillot, Salvatore Di Girolamo, Laureline Hentgen, Torsten Hoefler, Xavier Lapillonne, David Leutwyler, Katherine Osterried, Davide Panosetti, Stefan Rüdiger, Linda Schlemmer, Thomas C. Schulthess, Michael Sprenger, Stefano Ubiali, and Heini Wernli. 2020. Kilometer-Scale Climate Models: Prospects and Challenges. *Bulletin of the American Meteorological Society* 101, 5 (may 2020), E567–E587. <https://doi.org/10.1175/bams-d-18-0167.1>
- [26] Bjorn Stevens, Masaki Satoh, Ludovic Auger, Joachim Biercamp, Christopher S. Bretherton, Xi Chen, Peter Düben, Falko Judt, Marat Khairoutdinov, Daniel Klocke, Chihiro Kodama, Luis Kornbluh, Shian-Jiann Lin, Philipp Neumann, William M. Putman, Niklas Röber, Ryosuke Shibuya, Benoit Vanniere, Pier Luigi Vidale, Nils Wedi, and Linjiong Zhou. 2019. DYAMOND: the Dynamics of the Atmospheric general circulation Modeled On Non-hydrostatic Domains. *Progress in Earth and Planetary Science* 6, 1 (2019), 61. <https://doi.org/10.1186/s40645-019-0304-z>
- [27] Jian Sun, John M. Dennis, Sheri A. Mickelson, Brian Vanderwende, Andrew Gettelman, and Katherine Thayer-Calder. 2023. Acceleration of the Parameterization of Unified Microphysics Across Scales (PUMAS) on the Graphics Processing Unit (GPU) With Directive-Based Methods. *Journal of Advances in Modeling Earth Systems* 15, 5 (may 2023). <https://doi.org/10.1029/2022ms003515>

- [28] PyTorch team. 2023. TorchInductor: a PyTorch-native Compiler. <https://dev-discuss.pytorch.org/t/torchinductor-a-pytorch-native-compiler-with-define-by-run-ir-and-symbolic-shapes/747> [accessed 28-November-2023].
- [29] Inc. The Khronos Group. 2023. SYCL 2020 standard - language restrictions. https://registry.khronos.org/SYCL/specs/sycl-2020/html/sycl-2020.html#_language_restrictions_in_kernels [accessed 21-November-2023].
- [30] Inc. The Khronos Group. 2023. SYCL: a cross-platform abstraction layer for heterogeneous computing. <https://www.khronos.org/sycl> [accessed 30-November-2023].
- [31] Philippe Tillet, H. T. Kung, and David Cox. 2019. Triton: an intermediate language and compiler for tiled neural network computations. In *Proceedings of the 3rd ACM SIGPLAN International Workshop on Machine Learning and Programming Languages (PLDI '19)*. ACM. <https://doi.org/10.1145/3315508.3329973>
- [32] Christian R. Trott, Damien Lebrun-Grandie, Daniel Arndt, Jan Ciesko, Vinh Dang, Nathan Ellingwood, Rahul Kumar Gayatri, Evan Harvey, Daisy S. Hollman, Dan Ibanez, Nevin Liber, Jonathan Madsen, Jeff Miles, David Poliakoff, Amy Powell, Sivasankaran Rajamanickam, Mikael Simberg, Dan Sunderland, Bruno Turcksin, and Jeremiah Wilke. 2022. Kokkos 3: Programming Model Extensions for the Exascale Era. *IEEE Transactions on Parallel and Distributed Systems* 33, 4 (apr 2022), 805–817. <https://doi.org/10.1109/tpds.2021.3097283>
- [33] Jovan Đukić and Marko Mišić. 2023. An Evaluation of Directive-Based Parallelization on the GPU Using a Parboil Benchmark. *Electronics* 12, 22 (nov 2023), 4555. <https://doi.org/10.3390/electronics12224555>
- [34] R. Usha, Prachi Pandey, and N. Mangala. 2020. A Comprehensive Comparison and Analysis of OpenACC and OpenMP 4.5 for NVIDIA GPUs. In *2020 IEEE High Performance Extreme Computing Conference (HPEC)*. IEEE. <https://doi.org/10.1109/hpec43674.2020.9286203>

A CODE


```

1  template <DG> using DGVec = Eigen::Matrix<T, Eigen::Dynamic, DG>;
2
3  template <int CG, int DGstress, int DGadvection>
4  void StressUpdateHighOrder(const VPPParameters& vpparameters,
5      const ParametricMomentumMap<CG>& pmap, const ParametricMesh& smesh,
6      DGVec<DGstress>& S11, DGVec<DGstress>& S12, DGVec<DGstress>& S22,
7      const DGVec<DGstress>& E11, const DGVec<DGstress>& E12, const DGVec<DGstress>& E22,
8      const DGVec<DGadvection>& H, const DGVec<DGadvection>& A, double alpha, double beta)
9  {
10     constexpr int NGP = ((DGstress == 8) || (DGstress == 6)) ? 3 : (DGstress == 3 ? 2 : -1);
11     using EdgeVec = Eigen::Matrix<T, 1, NGP * NGP>;
12
13     #pragma omp parallel for
14     for (size_t i = 0; i < smesh.nelements; ++i) {
15         auto hGauss = (H.row(i) * PSI<DGadvection, NGP>).array().max(0.0).matrix();
16         auto aGauss = (A.row(i) * PSI<DGadvection, NGP>).array().max(0.0).min(1.0).matrix();
17         EdgeVec P = (_vpparameters.Pstar * hGauss.array()
18             * (-20.0 * (1.0 - aGauss.array())).exp()).matrix();
19
20         const EdgeVec e11Gauss = E11.row(i) * PSI<DGstress, NGP>;
21         const EdgeVec e12Gauss = E12.row(i) * PSI<DGstress, NGP>;
22         const EdgeVec e22Gauss = E22.row(i) * PSI<DGstress, NGP>;
23         const auto DELTA = (vpparameters.DeltaMin * vpparameters.DeltaMin
24             + 1.25 * (e11Gauss.array().square() + e22Gauss.array().square())
25             + 1.50 * e11Gauss.array() * e22Gauss.array()
26             + e12Gauss.array().square()).sqrt().matrix();
27
28         const T alphaInv = 1.0 / alpha;
29         const T fac = 1.0 - alphaInv;
30         const EdgeVec PDelta = P.array() / DELTA.array();
31         S11.row(i) = fac * S11.row(i) + (pmap.iMJwPSI[i]
32             * (alphaInv * (PDelta.array()
33                 * ((5.0 / 8.0) * e11Gauss.array() + (3.0 / 8.0) * e22Gauss.array())
34                 - 0.5 * P.array()).matrix().transpose()).transpose());
35         S12.row(i) = fac * S12.row(i) + (pmap.iMJwPSI[i]
36             * (alphaInv * (PDelta.array() * (1.0 / 4.0) * e12Gauss.array()
37                 .matrix().transpose()).transpose());
38         S22.row(i) = fac * S22.row(i) + (pmap.iMJwPSI[i]
39             * (alphaInv * (PDelta.array()
40                 * ((5.0 / 8.0) * e22Gauss.array() + (3.0 / 8.0) * e11Gauss.array())
41                 - 0.5 * P.array()).matrix().transpose()).transpose());
42     }
43 }

```

Listing 2: Implementation of the stress update with Eigen. The method is generic in the degrees of freedom of the different cG and dG elements. The matrix() and array() methods change the type of an expression to differentiate between matrix and component-wise operations and are no-ops during runtime.